PROCEEDINGS OF SCIENCE

Baryon-Electric Charge Correlations and Chemical Potentials as Probes of Magnetized QCD

Heng-Tong Ding, Jin-Biao Gu,* Arpith Kumar, Sheng-Tai Li and Jun-Hong Liu

Key Laboratory of Quark and Lepton Physics (MOE) and Institute of Particle Physics, Central China Normal University, Wuhan 430079, China

E-mail: jinbiaogu@mails.ccnu.edu.cn

We present the first lattice QCD results of quadratic fluctuations and correlations of conserved charges in (2+1)-flavor lattice QCD in the presence of a background magnetic field. The simulations were performed using the Highly Improved Staggered Quarks with physical pion mass m_π = 135 MeV on N_τ = 8 and 12 lattices. We find that the correlation between net baryon number and electric charge, denoted as $\chi_{11}^{\rm BQ}$, can serve as a magnetometer of QCD. At pseudocritical temperatures (T_{pc}) the $\chi_{11}^{\rm BQ}$ starts to increase rapidly with magnetic field strength $eB \gtrsim 2M_\pi^2$ and by a factor 2 at $eB \simeq 8M_\pi^2$. By comparing with the hadron resonance gas model, we find that the eB dependence of $\chi_{11}^{\rm BQ}$ is mainly due to the doubly charged $\Delta(1232)$ baryon. Although the doubly charged $\Delta(1232)$ could not be detected experimentally, its decay products, protons and pions, retain the eB dependence of $\Delta(1232)$'s contribution to $\chi_{11}^{\rm BQ}$. Furthermore, the ratio of electric charge chemical potential to baryon chemical potential, $\mu_{\rm Q}/\mu_{\rm B}$, shows significant dependence on the magnetic field strength and varies with the ratio of electric charge to baryon number in the colliding nuclei in heavy ion collisions. These results provide baselines for effective theory and model studies, and both $\chi_{11}^{\rm BQ}$ and $\mu_{\rm Q}/\mu_{\rm B}$ could be useful probes for the detection of magnetic fields in relativistic heavy ion collision experiments as compared with corresponding results from the hadron resonance gas model.

The 41st International Symposium on Lattice Field Theory (LATTICE2024)
28 July - 3 August 2024
Liverpool, UK

*Speaker

© Copyright owned by the author(s) under the terms of the Creative Commons Attribution-NonCommercial-NoDerivatives 4.0 International License (CC BY-NC-ND 4.0).

PoS(LATTICE2024)191

1. Introduction

Strong magnetic fields, conjectured to exist in relativistic heavy-ion collisions [1–3], magnetars [4], and the early universe [5], play a pivotal role in governing the behavior of quantum chromodynamics (QCD) matter. Model estimates suggest that the initial magnetic fields produced in non-central heavy-ion collisions at RHIC and the LHC may reach magnitudes of $eB \sim 5\ M_\pi^2$ and $eB \sim 70\ M_\pi^2$, respectively [2, 3]. Such intense fields are expected to significantly modify QCD interactions and leave detectable signatures on final-state observables [6].

The most prominent effect introduced by strong magnetic fields is the chiral magnetic effect (CME)[7], which has attracted intense theoretical and experimental interest [8]. The key to the CME lies in the strength and longevity of the magnetic field. However, a critical unresolved question is whether the transient field produced in heavy-ion collisions persists long enough to imprint measurable effects on the final-state particles. While first-principles lattice QCD studies have identified observables exhibiting strong dependence on magnetic fields, such as the splitting between u and d quark chiral condensates under external magnetic fields [9], these quantities remain experimentally inaccessible.

Fluctuations of and correlations among net baryon number (B), electric charge (Q), and strangeness (S) have long served as powerful tools to probe the QCD phase structure[10–13]. However, studies of these fluctuations under the presence of magnetic fields remain sparse and largely confined to effective models, like hadron resonance gas (HRG) [14–17], Polyakov-Nambu-Jona-Lasinio model (PNJL) [18]. First-principles lattice QCD calculations are essential to establish model-independent benchmarks. The lattice QCD investigation of fluctuations of conserved charges in external magnetic fields has been conducted with an unphysical pion mass ($M_\pi \simeq 220$ MeV) and a single lattice spacing in $N_f = 2+1$ QCD [19] , and more recently at the physical point in $N_f = 2+1+1$ QCD on $N_\tau = 8$ lattices [20].

In this work, we present the first (2+1)-flavor lattice QCD investigation of quadratic fluctuations and charge correlations in a background magnetic field with the physical pion mass. Our results establish model-independent benchmarks and reveal a significant enhancement of both the baryon electric charge correlations, χ_{11}^{BQ} and the ratio of electric charge chemical potential over baryon chemical potential, $\mu_{\mathrm{Q}}/\mu_{\mathrm{B}}$ in the presence of a magnetic field. These quantities are promising candidates for probing magnetic fields in relativistic heavy-ion collisions. This proceeding is based on the work presented in Ref. [21, 22].

2. Fluctuations of conserved charges and hadron resonance gas model

The fluctuations and correlations of conserved charge can be obtained by taking the derivatives of pressure with respect to the chemical potentials from lattice calculation evaluated at vanishing chemical potentials,

$$\chi_{ijk}^{\mathrm{BQS}} = \left.\frac{\partial^{i+j+k} p/T^4}{\partial\hat{\mu}_{\mathrm{B}}^i \partial\hat{\mu}_{\mathrm{Q}}^j \partial\hat{\mu}_{\mathrm{S}}^k}\right|_{\hat{\mu}_{\mathrm{B,Q,S}}=0}, \tag{1}$$

where $\hat{\mu}_X \equiv \mu_X/T$ with $X = \{\mathrm{B}, \mathrm{Q}, \mathrm{S}\}$ and $p = \frac{T}{V}\ln Z\left(V, T, \mu_{\mathrm{B}}, \mu_{\mathrm{Q}}, \mu_{\mathrm{S}}, eB\right)$ denotes the pressure of the magnetized thermal medium.

PoS(LATTICE2024)191

In the hadron resonance gas model, the pressure arising from charged and neutral particles in the presence of a magnetic field can be expressed as follows[19, 23]

$$\frac{p_n}{T^4} = \frac{g_i m_i^2}{2(\pi T)^2} \sum_{n=1}^{\infty} (\pm 1)^{n+1} \frac{e^{n\mu_i/T}}{n^2} \mathrm{K}_2\left(\frac{n m_i}{T}\right), \tag{2}$$

$$\frac{p_c}{T^4} = \frac{|q_i| B}{2\pi^2 T^3} \sum_{s_z=-s_i}^{s_i} \sum_{l=0}^{\infty} \varepsilon_l \sum_{n=1}^{\infty} (\pm 1)^{n+1} \frac{e^{n\mu_i/T}}{n} \mathrm{K}_1\left(\frac{n\varepsilon_l}{T}\right), \tag{3}$$

where q_i, m_i, s_i and g_i are the charge, mass, spin and degeneracy factor of the particle i. B is the magnitude of the magnetic field pointing along the z direction. $\varepsilon_l = \sqrt{m_i^2 + 2|q_i| B (l + 1/2 - s_z)}$ are the energy levels of charged particles with l denotes the Landau level. n is the sum index in the Taylor expansion series. K_2 and K_1 are the second-order and first-order modified Bessel functions of the second kind, respectively. The "+" in the "±" corresponds to mesons (where s_i is an integer) while the "−" corresponds to baryons (where s_i is a half-integer).

The quadratic fluctuations of and correlations among conserved charge arising from can be expressed by,

$$\begin{aligned} \chi_2^X &= \frac{B}{2\pi^2 T^3} \sum_i |q_i| X_i^2 \sum_{s_z=-s_i}^{s_i} \sum_{l=0}^{\infty} f(\varepsilon_0), \\ \chi_{11}^{XY} &= \frac{B}{2\pi^2 T^3} \sum_i |q_i| X_i Y_i \sum_{s_z=-s_i}^{s_i} \sum_{l=0}^{\infty} f(\varepsilon_0), \end{aligned} \tag{4}$$

where $f(\varepsilon_0) = \varepsilon_0 \sum_{n=1}^{\infty} (\pm 1)^{n+1} n \, \mathrm{K}_1\left(\frac{n\varepsilon_0}{T}\right)$ and $X_i, Y_i = \mathrm{B}_i, \mathrm{Q}_i, \mathrm{S}_i$ carried by hadron i. In this work, we focus on the computation of quadratic fluctuations and correlations, i.e. $i + j + k = 2$.

3. Lattice setup

In this work, we adopt the highly improved staggered quarks (HISQ) [24] and a tree-level improved Symanzik gauge action to perform lattice simulations of $N_f = 2 + 1$ QCD in external magnetic fields [19]. We primarily use the results from $32^3 \times 8$ and $48^3 \times 12$ lattices to perform continuum estimate. To validate the reliability of our continuum estimate results, we have conducted additional measurements at a specific temperature and magnetic field value on $64^3 \times 16$ lattice. The constant magnetic field is introduced along the z-direction and is described by a fixed factor $u_\mu(n)$ of the $U(1)$ field, which defined within the Landau gauge framework [25, 26],

$$\begin{aligned} u_x(n_x, n_y, n_z, n_\tau) &= \begin{cases} \exp\left[-ia^2 q B N_x n_y\right] & (n_x = N_x - 1) \\ 1 & (\text{otherwise}) \end{cases} \\ u_y(n_x, n_y, n_z, n_\tau) &= \exp\left[ia^2 q B n_x\right], \\ u_z(n_x, n_y, n_z, n_\tau) &= u_t(n_x, n_y, n_z, n_\tau) = 1, \end{aligned} \tag{5}$$

Unlike our previous studies [19], the quark masses are now fixed to their physical values, corresponding to a pion mass of $M_\pi = 135$ MeV in the absence of a magnetic field. Our temperature range is centered around T_{pc}, spanning from $0.9T_{pc}$ to $1.1T_{pc}$. To mimic the intense magnetic fields generated during the initial stages of relativistic heavy-ion collisions, we implemented six distinct values of magnetic field strengths eB up to $8M_\pi^2$.

PoS(LATTICE2024)191

4. Results and discussions

For obtaining the continuum estimate, we perform a joint fit using a linear extrapolation in terms of $1/N_\tau^2$,

$$O\left(T, eB, N_\tau\right) = O(T, eB) + \frac{c}{N_\tau^2}, \tag{6}$$

where $O(T, eB)$ is the final continuum estimate.

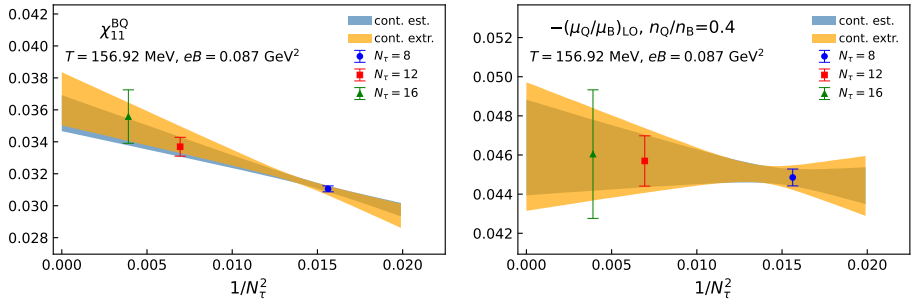

Figure 1: Continuum estimate (blue band) and extrapolation (yellow band) result of χ_{11}^{BQ} (left) and $-\left(\mu_{\mathrm{Q}}/\mu_{\mathrm{B}}\right)_{\mathrm{LO}}$ with $n_{\mathrm{Q}}/n_{\mathrm{B}} = 0.4$ (right) at $T = 156.92$ MeV at $eB = 0.087$ GeV^2. The points for $N_\tau = 8$ and 12 are interpolated results while the point for $N_\tau = 16$ denotes the lattice data.

The left panel of Figure 1 shows the baryon electric charge correlation as a function of $1/N_\tau^2$ at specific temperature and magnetic field. We compare the continuum estimates obtained using $N_\tau = \{8, 12\}$ with the continuum extrapolation derived from $N_\tau = \{8, 12, 16\}$, and the systematic uncertainties between two methods are within the statistical uncertainties. The right panel presents analogous results for $\left(\mu_{\mathrm{Q}}/\mu_{\mathrm{B}}\right)_{\mathrm{LO}}$, a composite observable derived from six quadratic conserved charge fluctuations and correlations. These consistencies demonstrate the reliability of our continuum estimate method, even when applied to complex observables.

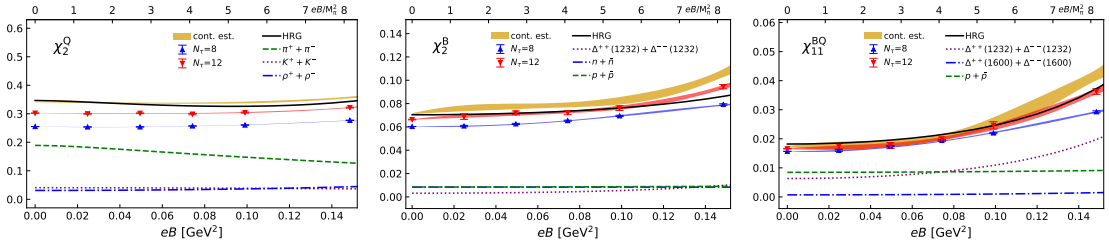

Figure 2: The yellow band represents the continuum estimates of χ_2^{Q}, χ_2^{B} and χ_{11}^{BQ} at non vanishing magnetic field with $T = 145$ MeV. The black solid line and broken line shows the total contribution and contributions from individual hadrons to χ_2^{Q}, χ_2^{B} and χ_{11}^{BQ} obtained from the HRG model.

Figure 2 shows the results of χ_2^{Q}, χ_2^{B} and χ_{11}^{BQ} as a function of magnetic field strength obtained from lattice QCD computation and HRG model at $T = 145$ MeV. The color bands in figure are obtained from B-spline interpolation on T-eB plane using data from various N_b and T values. Further interpolation details are provided in Ref. [22]. The lattice continuum estimates are obtained from the $N_\tau = 8$ and 12. We find χ_2^{Q} almost independent of eB. From the perspective of the HRG

PoS(LATTICE2024)191

model, this can be attributed to the counterbalancing of different hadronic contributions. With increasing of the magnetic field the contribution from half-spin meson, such as pions, decreases, while that from higher-spin hadrons increases. χ_2^{B} increase with eB, but the HRG model fails to capture this trend due to its assumption that the energies of neutral particles are not affected by magnetic fields. χ_{11}^{BQ} exhibits strikingly sensitivity to the magnetic field, reaching 2.4 times its value at vanishing magnetic field at $eB \simeq 8M_\pi^2$. Such a remarkable enhancement suggests its potential utility as a magnetometer in QCD. With the aid of the HRG model, we can discern that this significant increase is predominantly driven by the contributions from $\Delta^{++}(1232)$ ($\Delta^{--}(1232)$). However, doubly charged Δ baryons undergo strong decay and rapidly decay to stable particles such as protons and pions, which implies that they cannot be measured directly in heavy-ion collision (HIC) experiments.

Advantageously, Ref. [27] provides a method for reconstructing the contributions of resonances using stable particles within the HRG framework. Here we employ π, K and p to construct the proxies for the resonance contributions [28]. The proxy for χ_2^{Q} and χ_{11}^{BQ} are defined follows,

$$\begin{aligned}\sigma^{1,1}_{Q^{\mathrm{PID}},p} &= \sum_R \left(P_{R\to\tilde{p}}\right)\left(P_{R\to Q^{\mathrm{PID}}}\right) I_R^{\mathrm{BQ}} + I_{\tilde{p}}^{\mathrm{BQ}},\\ \sigma^{2}_{Q^{\mathrm{PID}}} &= \sum_R \left(P_{R\to Q^{\mathrm{PID}}}\right)^2 I_R^{\mathrm{Q}} + I_{Q^{\mathrm{PID}}}^{\mathrm{Q}},\end{aligned} \tag{7}$$

where $\tilde{j} = j - \bar{j}$ represents the net quantum number of particle species j,with $P_{R\to\tilde{j}} = P_{R\to j} - P_{R\to\bar{j}}$. $P_{R\to j} = \sum_\alpha N^\alpha_{R\to j} n^R_{j,\alpha}$ giving the average number of particle j produced by each particle R after the entire decay chain. α is a decay channel from R to j, $N^\alpha_{R\to j}$ is the branching ratio, and $n^R_{j,\alpha}$ is the number of stable particle j produced from this decay channel. And $Q^{\mathrm{PID}} = \tilde{p} + \tilde{K} + \tilde{\pi}$ represents the summation of contributions from net proton, pion and kaon. We assumed that the branching ratios are independent of the magnetic field and we used all decay modes listed in the Particle Data Group [29]. The I_R^{BQ} and I_R^{Q} stands for the contribution from the particle R to χ_{11}^{BQ} and χ_2^{Q}, respectively, where $\chi_{11}^{\mathrm{BQ}} \equiv \sum_i I_i^{\mathrm{BQ}}$ and $\chi_2^{\mathrm{Q}} \equiv \sum_i I_i^{\mathrm{Q}}$.

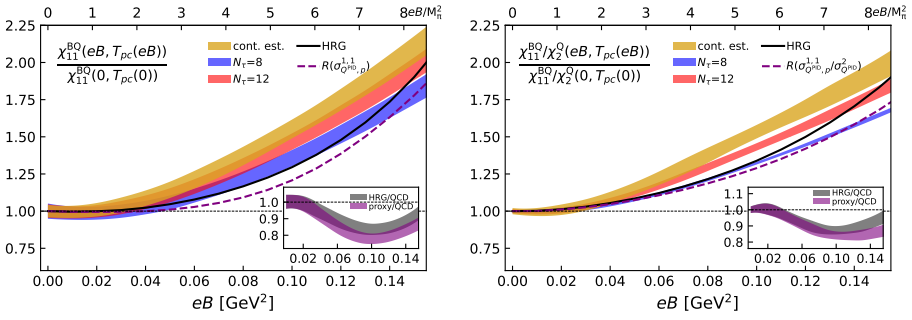

Figure 3: The R_{cp}-like ratios of χ_{11}^{BQ} and $\chi_{11}^{\mathrm{BQ}}/\chi_2^{\mathrm{Q}}$ from lattice QCD to their corresponding values at vanishing magnetic fields (yellow band) along the transition line. The results from HRG (black solid line) and proxy (purple dashed line) are also shown. The insets show the ratios of results calculated from HRG and proxy to lattice computation.

The pseudocritical temperature $T_{pc}(\sim 156\,\mathrm{MeV})$ is close to the chemical freeze out temperature in HIC experiments [30, 31]. In this context, weak magnetic fields correspond to the central

PoS(LATTICE2024)191

collisions, while strong magnetic fields correspond to the peripheral collisions. Therefore, the ratio of an observable at non-zero magnetic field to its value at vanishing magnetic field defines a R_{cp}-like observable. In Figure 3, we present R_{cp}-like ratios for χ_{11}^{BQ} and $\chi_{11}^{\mathrm{BQ}}/\chi_{2}^{\mathrm{Q}}$ along the transition line. It can be observed that the ratio of χ_{11}^{BQ} exhibits significant dependence on the magnetic field even at higher temperatures. While both the HRG model and the proxy can reproduce the lattice QCD results only within a limited range of magnetic field strengths,$\sim M_\pi^2$, the proxy retains the significant magnetic field dependence feature of χ_{11}^{BQ}. In the context of HIC experiments, double-ratio observables are commonly utilized to mitigate volume-dependent effects [28]. Notably, the proxy for $\chi_{11}^{\mathrm{BQ}}/\chi_{2}^{\mathrm{Q}}$ mirrors the behavior of χ_{11}^{BQ}, suggesting its viability as a probe for magnetic field effects [1].

The baryon chemical potential (μ_{B}) and the electric charge chemical potential (μ_{Q}) can be extracted via thermal statistical fits to the particle yields in experiments[31, 33, 34], while their ratio $\mu_{\mathrm{Q}}/\mu_{\mathrm{B}}$ is accessible through lattice QCD calculations. The electric charge chemical potential can be expanded as a series in terms of the μ_{B},

$$\mu_{\mathrm{Q}}/\mu_{\mathrm{B}} = q_1 + q_3\,\hat{\mu}_{\mathrm{B}}^2 + O(\hat{\mu}_{\mathrm{B}}^4), \tag{8}$$

where the leading-order (LO) coefficient q_1 can be expressed as,

$$q_1 = \frac{r\left(\chi_2^{\mathrm{B}}\chi_2^{\mathrm{S}} - \chi_{11}^{\mathrm{BS}}\chi_{11}^{\mathrm{BS}}\right) - \left(\chi_{11}^{\mathrm{BQ}}\chi_2^{\mathrm{S}} - \chi_{11}^{\mathrm{BS}}\chi_{11}^{\mathrm{QS}}\right)}{\left(\chi_2^{\mathrm{Q}}\chi_2^{\mathrm{S}} - \chi_{11}^{\mathrm{QS}}\chi_{11}^{\mathrm{QS}}\right) - r\left(\chi_{11}^{\mathrm{BQ}}\chi_2^{\mathrm{S}} - \chi_{11}^{\mathrm{BS}}\chi_{11}^{\mathrm{QS}}\right)}, \tag{9}$$

where $r = n_{\mathrm{Q}}/n_{\mathrm{B}}$ is the ratio of net electric charge to net baryon number density in the initial colliding nuclei. The next-to-leading order (NLO) coefficient expression can be found in Ref. [35].

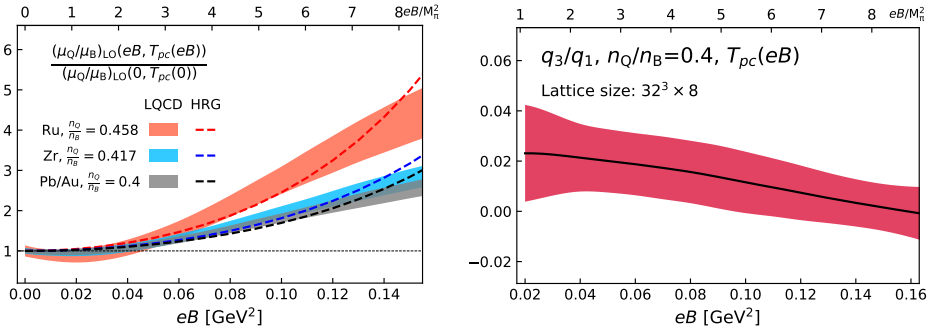

Figure 4: The left panel: the continuum estimated ratio of leading-order coefficient of $\mu_{\mathrm{Q}}/\mu_{\mathrm{B}}$ as a function of eB at T_{pc}. The right panel: the eB dependence of q_3/q_1 obtained on $32^3 \times 8$ lattices for $n_{\mathrm{Q}}/n_{\mathrm{B}} = 0.4$ at T_{pc}.

The left panel of Figure 4 illustrates the magnetic field dependence of the R_{cp}-like of q_1 for various colliding systems along the transition line. It can be seen that q_1 exhibits sensitivity not only to magnetic fields but also to the colliding nuclei involved in collisions. At $eB \sim 8M_\pi^2$, although the charge-to-mass ratio of the Ruthenium ($^{96}_{44}$Ru) collision system is only 10% larger than that for

[1] In the current work, the kinematic cuts in the proxy have not yet been adopted, and their impact will be investigated in future studies [32].

PoS(LATTICE2024)191

Zirconium ($^{96}_{40}$Zr), the ratio of q_1 in the $^{96}_{44}$Ru + $^{96}_{44}$Ru collision system exceeds that in the $^{96}_{40}$Zr + $^{96}_{40}$Zr by 50%. The right panel shows the ratio of NLO coefficient q_3 to LO coefficient q_1 as a function of eB, calculated on lattices with $N_\tau = 8$. The q_3/q_1 remains within approximately 5%. Furthermore, the discretization error for this quantity is minor [35, 36], indicating that higher-order corrections to μ_Q/μ_B in the continuum limit remain small. The pronounced enhancement under external eB further suggests that μ_Q/μ_B is well-suited to serve as a magnetometer in relativistic heavy ion collisions.

5. Conclusions

In this work, we have presented the first lattice QCD computations of the second order fluctuations of conserved charges in an external magnetic field with a physical pion mass. The continuum estimates are based on $N_\tau = 8$ and 12 lattices. We observe that both χ_{11}^{BQ} and μ_Q/μ_B are significantly influenced by eB, suggesting their potential utility as magnetometers for QCD. With the aid of the hadron resonance gas model, we can construct proxies for χ_{11}^{BQ} using detectable hadrons in HIC experiments, and these proxies still exhibit the strong dependence of χ_{11}^{BQ} on the magnetic field. To better align with the measurements in HIC experiments, future studies will incorporate kinematic cuts into the analysis of conserved charge fluctuations in the HRG framework [37]. On the other hand, the ratio of μ_Q/μ_B can also be obtained by thermal statistical fits to the particle yields experimentally. However, in such thermal fitting, an additional parameter eB is required to account for the influence of the magnetic field on hadron energies. Finally, our results also provide a QCD benchmark for second order fluctuations of conserved charges for effective theories and model studies.

Acknowledgments

This work was supported in part by the National Natural Science Foundation of China under Grants No. 12293064, No. 12293060, and No. 12325508, and the National Key Research and Development Program of China under Contract No. 2022YFA1604900. The numerical simulations were performed using the GPU cluster at the Nuclear Science Computing Center of Central China Normal University (NSC3) and the Wuhan Supercomputing Center.

References

[1] D.E. Kharzeev, L.D. McLerran and H.J. Warringa, *The Effects of topological charge change in heavy ion collisions: 'Event by event P and CP violation'*, *Nucl. Phys. A* **803** (2008) 227 [0711.0950].

[2] W.-T. Deng and X.-G. Huang, *Event-by-event generation of electromagnetic fields in heavy-ion collisions*, *Phys. Rev. C* **85** (2012) 044907 [1201.5108].

[3] V. Skokov, A.Y. Illarionov and V. Toneev, *Estimate of the magnetic field strength in heavy-ion collisions*, *Int. J. Mod. Phys. A* **24** (2009) 5925 [0907.1396].

PoS(LATTICE2024)191

[4] K. Enqvist and P. Olesen, *On primordial magnetic fields of electroweak origin*, *Phys. Lett. B* **319** (1993) 178 [hep-ph/9308270].

[5] T. Vachaspati, *Magnetic fields from cosmological phase transitions*, *Phys. Lett. B* **265** (1991) 258.

[6] D.E. Kharzeev, K. Landsteiner, A. Schmitt and H.-U. Yee, *'Strongly interacting matter in magnetic fields': an overview*, *Lect. Notes Phys.* **871** (2013) 1 [1211.6245].

[7] K. Fukushima, D.E. Kharzeev and H.J. Warringa, *The Chiral Magnetic Effect*, *Phys. Rev. D* **78** (2008) 074033 [0808.3382].

[8] D.E. Kharzeev and J. Liao, *Chiral magnetic effect reveals the topology of gauge fields in heavy-ion collisions*, *Nature Rev. Phys.* **3** (2021) 55 [2102.06623].

[9] H.T. Ding, S.T. Li, A. Tomiya, X.D. Wang and Y. Zhang, *Chiral properties of (2+1)-flavor QCD in strong magnetic fields at zero temperature*, *Phys. Rev. D* **104** (2021) 014505 [2008.00493].

[10] H.-T. Ding, F. Karsch and S. Mukherjee, *Thermodynamics of strong-interaction matter from Lattice QCD*, *Int. J. Mod. Phys.* **E24** (2015) 1530007 [1504.05274].

[11] W.-j. Fu, *QCD at finite temperature and density within the fRG approach: An overview*, 2205.00468.

[12] X. Luo and N. Xu, *Search for the QCD Critical Point with Fluctuations of Conserved Quantities in Relativistic Heavy-Ion Collisions at RHIC : An Overview*, *Nucl. Sci. Tech.* **28** (2017) 112 [1701.02105].

[13] A. Pandav, D. Mallick and B. Mohanty, *Search for the QCD critical point in high energy nuclear collisions*, *Prog. Part. Nucl. Phys.* **125** (2022) 103960 [2203.07817].

[14] K. Fukushima and Y. Hidaka, *Magnetic Shift of the Chemical Freeze-out and Electric Charge Fluctuations*, *Phys. Rev. Lett.* **117** (2016) 102301 [1605.01912].

[15] M. Ferreira, P. Costa and C. Providência, *Net baryon-number fluctuations in magnetized quark matter*, *Phys. Rev. D* **98** (2018) 034003 [1806.05758].

[16] A. Bhattacharyya, S.K. Ghosh, R. Ray and S. Samanta, *Exploring effects of magnetic field on the Hadron Resonance Gas*, *EPL* **115** (2016) 62003 [1504.04533].

[17] G. Kadam, S. Pal and A. Bhattacharyya, *Interacting hadron resonance gas model in magnetic field and the fluctuations of conserved charges*, *J. Phys. G* **47** (2020) 125106 [1908.10618].

[18] W.-j. Fu, *Fluctuations and correlations of hot QCD matter in an external magnetic field*, *Phys. Rev. D* **88** (2013) 014009 [1306.5804].

[19] H.T. Ding, S.T. Li, Q. Shi and X.D. Wang, *Fluctuations and correlations of net baryon number, electric charge and strangeness in a background magnetic field*, *Eur. Phys. J. A* **57** (2021) 202 [2104.06843].

PoS(LATTICE2024)191

[20] S. Borsanyi, B. Brandt, G. Endrodi, J. N. Guenther, R. Kara and A.D. Marques Valois, *QCD equation of state in the presence of magnetic fields at low density*, *PoS* **LATTICE2023** (2024) 164 [2312.15118].

[21] H.-T. Ding, S.-T. Li, J.-H. Liu and X.-D. Wang, *Fluctuations of Conserved Charges in Strong Magnetic Fields from Lattice QCD*, *Acta Phys. Polon. Supp.* **16** (2023) 1 [2208.07285].

[22] H.-T. Ding, J.-B. Gu, A. Kumar, S.-T. Li and J.-H. Liu, *Baryon Electric Charge Correlation as a Magnetometer of QCD*, *Phys. Rev. Lett.* **132** (2024) 201903 [2312.08860].

[23] HotQCD collaboration, *Fluctuations and Correlations of net baryon number, electric charge, and strangeness: A comparison of lattice QCD results with the hadron resonance gas model*, *Phys. Rev. D* **86** (2012) 034509 [1203.0784].

[24] HPQCD, UKQCD collaboration, *Highly improved staggered quarks on the lattice, with applications to charm physics*, *Phys. Rev.* **D75** (2007) 054502 [hep-lat/0610092].

[25] G.S. Bali, F. Bruckmann, G. Endrodi, Z. Fodor, S.D. Katz, S. Krieg et al., *The QCD phase diagram for external magnetic fields*, *JHEP* **02** (2012) 044 [1111.4956].

[26] M. Al-Hashimi and U.-J. Wiese, *Discrete Accidental Symmetry for a Particle in a Constant Magnetic Field on a Torus*, *Annals Phys.* **324** (2009) 343 [0807.0630].

[27] R. Bellwied, S. Borsanyi, Z. Fodor, J.N. Guenther, J. Noronha-Hostler, P. Parotto et al., *Off-diagonal correlators of conserved charges from lattice QCD and how to relate them to experiment*, *Phys. Rev. D* **101** (2020) 034506 [1910.14592].

[28] STAR collaboration, *Collision-energy dependence of second-order off-diagonal and diagonal cumulants of net-charge, net-proton, and net-kaon multiplicity distributions in Au + Au collisions*, *Phys. Rev. C* **100** (2019) 014902 [1903.05370].

[29] Particle Data Group collaboration, *Review of Particle Physics*, *PTEP* **2020** (2020) 083C01.

[30] HotQCD collaboration, *Chiral crossover in QCD at zero and non-zero chemical potentials*, *Phys. Lett. B* **795** (2019) 15 [1812.08235].

[31] ALICE collaboration, *Production of ^{4}He and $^4\overline{\text{He}}$ in Pb-Pb collisions at $\sqrt{s_{\text{NN}}} = 2.76$ TeV at the LHC*, *Nucl. Phys. A* **971** (2018) 1 [1710.07531].

[32] H.-T. Ding, J.-B. Gu, A. Kumar and S.-T. Li, *work in progress*, .

[33] P. Braun-Munzinger, K. Redlich and J. Stachel, *Particle production in heavy ion collisions*, nucl-th/0304013.

[34] STAR collaboration, *Bulk Properties of the Medium Produced in Relativistic Heavy-Ion Collisions from the Beam Energy Scan Program*, *Phys. Rev. C* **96** (2017) 044904 [1701.07065].

PoS(LATTICE2024)191

[35] A. Bazavov, H.-T. Ding, P. Hegde et al., *The QCD Equation of State to $O(\mu_B^6)$ from Lattice QCD*, *Phys. Rev.* **D95** (2017) 054504 [1701.04325].

[36] A. Bazavov, H.-T. Ding, P. Hegde, O. Kaczmarek, F. Karsch et al., *Freeze-out Conditions in Heavy Ion Collisions from QCD Thermodynamics*, *Phys.Rev.Lett.* **109** (2012) 192302 [1208.1220].

[37] F. Karsch, K. Morita and K. Redlich, *Effects of kinematic cuts on net-electric charge fluctuations*, *Phys. Rev. C* **93** (2016) 034907 [1508.02614].

PoS(LATTICE2024)191